

# 碳纳米管堆积床导热及热松弛

阚伟民<sup>1</sup>, 章先涛<sup>2</sup>, 肖小清<sup>1</sup>, 程 婷<sup>2</sup>

(1. 广东电力科学研究院 广东 广州 510600; 2. 武汉大学 动力与机械学院 湖北 武汉 430072)

**摘 要:** 运用热线法测量了碳纳米管堆积床在 120 K - 370 K 温度范围内的导热系数和传热松弛时间。测量数据表明: 碳纳米管床导热系数极低, 其在低温段随温度升高呈线性增加, 在高于室温的范围趋于稳定。测量过程中碳纳米管床表现出的传热松弛时间, 较已有文献报道的最大的碳纳米管床传热松弛时间大一个数量级。基于此数据并结合经典的 ( CV 双曲型热传导) 模型分析单个碳纳米管接触节点上的瞬态导热及热电特性, 分析认为: 利用纳米多孔材料的传热延迟特性可提高瞬态热电转换效率。

**关 键 词:** 纳米复合材料; 碳纳米管床; 松弛时间; 导热系数; 热电

中图分类号: TK124 文献标识码: A

符号说明:

- $A$ —基本单元垂直于热流方向的有效面积 /  $m^2$
- $b$ —探针温升与时间在对数坐标下的斜率
- $C$ —空气的体积比热容 /  $kJ \cdot kg^{-1}$
- $D$ —碳纳米管床单元格有效特征尺寸 /  $m$
- $d$ —碳管直径 /  $mm$
- $G$ —导热系数 /  $W \cdot (m \cdot K)^{-1}$
- $k$ —材料导热系数 /  $W \cdot (m \cdot K)^{-1}$
- $l$ —碳管长度 /  $nm$
- $n$ —碳管的数密度
- $Q$ —热流 /  $W$
- $q_0$ —探针加热线功率 /  $W$
- $r$ —柱坐标的径向坐标
- $r_0$ —探针半径 /  $mm$
- $T$ —探针温度 /  $K$
- $T_0$ —样品初始温度 /  $K$
- $T_1$ —碳管 1 温度 /  $K$
- $T_2$ —碳管 2 温度 /  $K$
- $t$ —时间 /  $s$
- $a$ —热扩散系 /  $m^2 \cdot s^{-1}$
- $\gamma$ —欧拉常数
- $L$ —空气在碳纳米管床中的平均自由程 /  $m$
- $n$ —声速 /  $m \cdot s^{-1}$
- $r$ —密度 /  $kg \cdot m^{-3}$
- $r_{CNT}$ —碳管密度 /  $kg \cdot m^{-3}$
- $\tau$ —松弛时间 /  $s$

## 引 言

纳米复合材料不但具有固体的力学特性且具有非常低的导热系数<sup>[1-3]</sup>, 因此它在很多工程中如高温能量储存、汽轮机和热电转化技术上都有极大的应用前景<sup>[4-5]</sup>。纳米复合材料由于制造简单、价格低廉在生产应用上相比于其它纳米结构热电材料 (如纳米薄膜、超晶格以及纳米线<sup>[6-9]</sup>) , 在热电应用方面具有更大的优势<sup>[10-13]</sup>。

无论对于储能性能还是对于热电性能, 材料的导热系数都是至关重要的参数。而大部分纳米复合材料导热系数决定于固体纳米框架的导热系数。由于纳米颗粒之间存在巨大的接触热阻, 固体纳米框架导热系数主要受纳米颗粒间接触热阻限制, 而与纳米颗粒本身的导热系数几乎无关<sup>[14-16]</sup>。基于上述考虑纳米颗粒接触热阻的模型被提出用来分析纳米颗粒框架的有效导热系数<sup>[17-19]</sup>。此前所有的研究集中在纳米复合材料的稳态导热性能上, 然而对其瞬态热性能的研究鲜有报道。本研究以碳纳米管堆积床为研究对象, 采用热线法测量并获得了碳纳米管床在 120 - 370 K 的温度范围内的导热系数和导热松弛时间, 在此基础上提出一个考虑松弛时间的导热模型研究碳纳米管之间的瞬态导热及热电现象。

## 1 实验

### 1.1 实验装置及材料

实验采用商用多壁碳纳米管颗粒, 直径 20 - 40 nm, 长度的 5  $\mu m$ 。碳纳米管以一定密度 (195  $kg/m^3$ ) 堆积在玻璃容器中, 玻璃容器直径为 3 cm。采用热线法测量碳纳米管堆积床的瞬态导热特性, 热线探针垂直置于样品中间。装样品的玻璃容器整体

收稿日期: 2013 - 11 - 05

基金项目: 国家自然科学基金 (50906064); 教育部博士点基金 (20100141110022)

作者简介: 阚伟民 (1969 -), 男, 湖北咸宁人, 广东电力科学研究院高级工程师。

置于一个封闭容器内,以控制测量温度在 120 – 370 K 温度范围,实验装置如图 1 所示。所用探针直径为 1 mm,长度 4 cm,探针内放置均匀的加热丝及存于探针中间的热电偶用以监测样品在被恒定热流加热时的温度变化。在每一次的测量中,探针的温升为 2 – 3 °C,温度测量误差 ±0.2 °C 范围内。每次加热持续时间控制在 20 s 左右,以保证材料内部温升未传递到容器壁面。

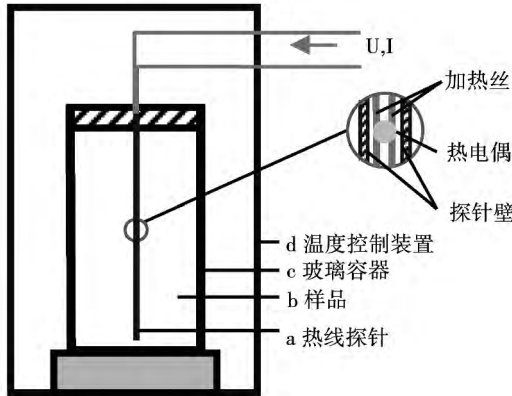


图 1 实验装置图

Fig. 1 Drawing of the test device

### 1.2 数据处理

将探针温升的理论解拟合实验数据可得到被测材料的热物性,求解坐标下经典瞬态导热方程可得到探针温升的解为:

$$T = \frac{q_0}{4\pi k} [\ln(\frac{r_0^2}{4\alpha t}) + \gamma] \quad (1)$$

根据式 (1) 可得到传统热线法测导热系数的公式:

$$k = q_0 / (4pb) \quad (2)$$

拟合结果显示,基于傅里叶定律的经典瞬态导热方程得到的解与实验结果无法拟合,如图 2 所示。基于式 (2) 得到的  $k$  值或由稳态法测得的  $k$  值,式 (1) 的理论预测值均远高于实验值。考虑多孔体里存在大松弛时间的经典现象也可能适用于碳纳米管堆积床,因此采用考虑松弛时间的双曲热传导方程对实验结果进行分析:

$$\alpha \left[ \frac{\partial^2 T(r,t)}{\partial r^2} + \frac{1}{r} \frac{\partial T(r,t)}{\partial r} \right] = \frac{\partial T(r,t)}{\partial t} + \tau \frac{\partial^2 T(r,t)}{\partial t^2} \quad (3)$$

方程的边界条件为:

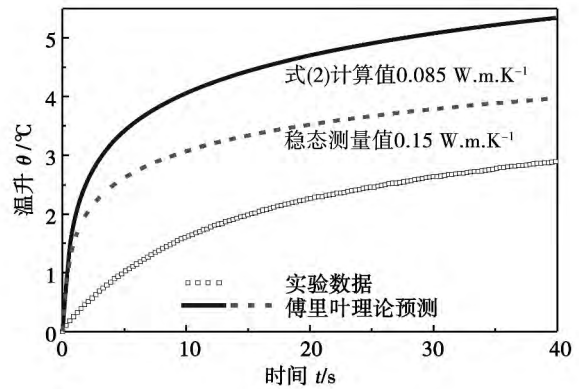


图 2 实验结果与基于傅里叶定律理论预测的比较

Fig. 2 Comparison of the test results with those predicted by using the theory based on Fourier law

$$T(r, \rho) = T_0, \frac{\partial T}{\partial t} \Big|_{t=0} = 0, k \frac{\partial T}{\partial r} \Big|_{r_0} = q_0 \quad (4)$$

式中:  $T_0$ —样品的初始温度,求解方程 (3),在  $r = r_0$  处<sup>[20]</sup>

$$T(t) = T_0 + \frac{q_0 r_0}{k} \times$$

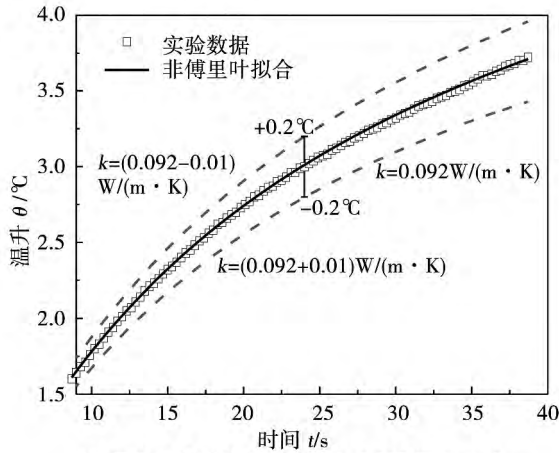
$$\left( \frac{1}{\pi} \int_0^{1/\Xi} \frac{J_1(\rho(y)) Y_0(\rho(y)) - Y_1(\rho(y)) J_0(\rho(y))}{\rho(y) (J_1(\rho(y))^2 + Y_1(\rho(y))^2)} \times \psi(y, \xi) dy + \int_{1/\Xi}^{\infty} \frac{I_1(\rho(y)) K_0(\rho(y)) - K_1(\rho(y)) I_0(\rho(y))}{\rho(y) (\pi^2 I_1(\rho(y))^2 + K_1(\rho(y))^2)} \times \psi(y, \xi) dy \right) \quad (5)$$

式中:  $\rho(y) = \sqrt{(y \cdot |1 - \Xi y|)}$ ,  $\psi(y, \xi) = e^{-y\xi} \int_0^\xi e^{\lambda y} g(\lambda) d\lambda$ ,  $\xi = \alpha t / r_0^2$ ,  $\Xi = \alpha \tau / r_0^2$ 。通过最小二乘法以式 (5) 拟合实验测得的温升曲线可分别得到  $k$  和  $\tau$ 。图 3 为样品在 180 K 时的测量及拟合结果,从图中可以看出  $k$  和  $\tau$  的取值的不同对温度变化曲线产生不同的影响,  $k$  的变化主要影响的是曲线的形状,  $\tau$  的变化主要影响的是曲线的位置,因此  $k$  与  $\tau$  之间相互几乎没有影响。考虑到热电偶测量温度的误差是在 ±0.2 °C 的范围之内,由此所产生的  $k$  和  $\tau$  的拟合误差分别小于 10% 和 30%,如图 3 所示。

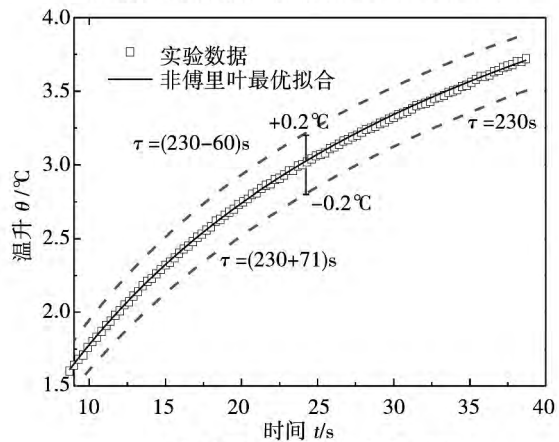
## 2 实验结果与讨论

为验证数据处理方法的可靠性,在室温下测量 3 个不同孔隙率的样品的导热系数并将拟合得到的

结果与室温下稳态方法的实验结果进行比较,如图 4 所示。不考虑松弛时间的式(2)的拟合结果明显低于稳态值,而考虑松弛时间的式(5)则与稳态测量结果一致,由此可见,用考虑松弛时间的式(5)拟合实验结果可得到材料真实导热系数。



(a) 导热系数拟合曲线 最佳 $k=0.092 \text{ W}/(\text{m} \cdot \text{K})$



(b) 松弛时间拟合曲线 最佳 $\tau=230 \text{ s}$

图 3 导热系数和松弛时间的最优拟合  
Fig. 3 Optimum fitting of the heat conduction coefficient and the relaxation time

图 5 为利用式(5)拟合得到的碳纳米管堆积床从 120 – 370 K 温度范围内的导热系数。在低于室温段样品导热系数随温度提高几乎呈线性增加,而在高于室温段基本保持不变。由于碳纳米管床的导热系数由碳纳米管之间的巨大接触热阻所决定,导热系数的变化趋势将随碳纳米管间的热导变化而定。对于碳纳米管堆积床,管床的导热系数与碳纳米管之间热导系数  $G$  的关系为<sup>[17]</sup>:

$$k_{\text{network}} = \frac{G}{d} \frac{\pi n^2}{18} \left[ 1 + 16 \frac{d}{2l} + 80 \left( \frac{d}{2l} \right)^2 + 192 \left( \frac{d}{2l} \right)^3 + 153.6 \left( \frac{d}{2l} \right)^4 \right] \quad (6)$$

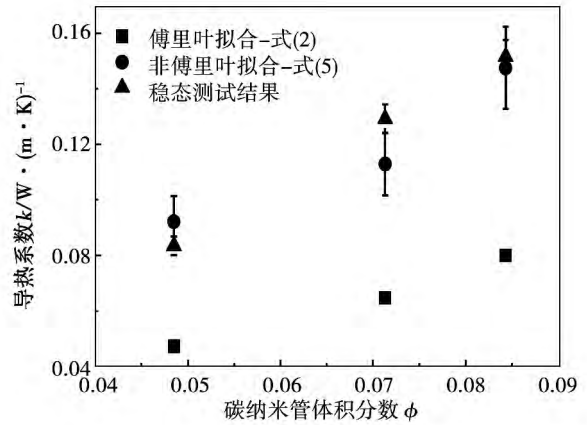
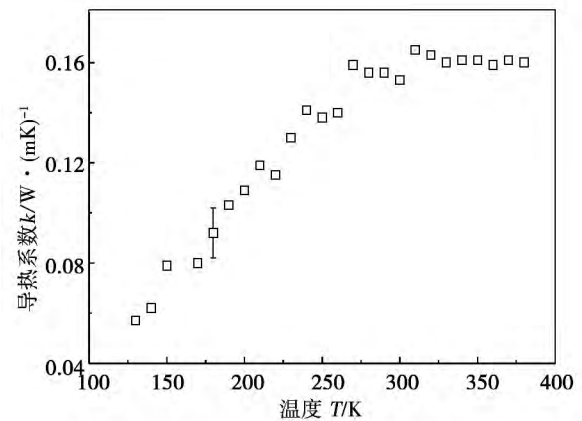


图 4 由式(2)和式(5)拟合得到的热线法测量结果与瞬态测量结果的比较

Fig. 4 Comparison of the results measured by using the hot wire method and obtained by fitting based on the formula No. 2 and 5 with those measured in the transient state



(a) 碳纳米管床导热系数随温度的变化

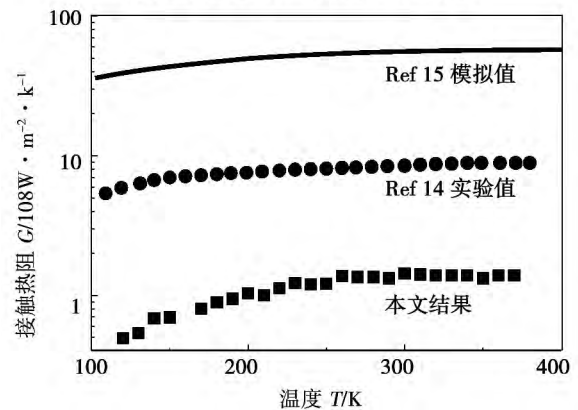


图 5 样品密度为  $195 \text{ kg}/\text{m}^3$  碳纳米管床导热系数随温度的变化

Fig. 5 Changes of the heat conduction coefficient of a nanometer carbon tube bed, of which the density of the sample is  $195 \text{ kg} \cdot \text{m}^{-3}$ , with temperature

式中:  $d$ —碳纳米管的直径(取 30 nm)  $l$ —碳纳米管的长度(取 5 mm)。其中  $\bar{n} = 0.5 nl^2 d$  是无量纲密度  $n$  是碳管的数密度。由于测试样品体积分数较低(9.3%) ,须考虑空气的影响。碳纳米管床的有效导热系数由碳纳米管床固体架构的导热与空气导热两部分决定:  $k_{\text{effective}} = k_{\text{network}} + (1 - \phi) k_{\text{air}}$ 。其中  $\phi$  是碳纳米管的体积分数  $k_{\text{air}}$  是空气的导热系数 等于  $1/3 C v \Lambda$  其中  $\Lambda$  是空气在碳纳米管床中的平均有效自由程,可由马西森定律法则计算:  $1/\Lambda = 1/\Lambda_{\text{air}} + 1/D$ ,  $C$  是空气的体积比热容  $v$  是声速  $D = 3/4 \pi d^2 \rho_{\text{CNT}}/\rho$  为碳纳米管床单元格有效特征尺寸 其中  $\rho_{\text{CNT}}$  为碳管密度(取  $2\ 300\ \text{kg}/\text{m}^3$ )。通过计算发现,由于  $D$  在纳米量级,决定空气导热系数很小,基本可忽略不计。通过方程(6)和导热系数结果可以得到不同温度下碳纳米管之间的热导。如图 5 中的小图所示,热导在测量温度范围内与碳纳米管床导热系数随温度变化趋势一致,这与文献<sup>[14]</sup>中实验测得的单个多壁碳纳米管接触节点之间热导的测量结果十分吻合。

假设碳纳米管与碳管之间的接触面积和接触碳纳米管的直径的乘积成正比,可将本实验所得到的碳管接触节点单位面积热导值和文献中分子动力学模拟结果及实验结果进行比较。如图 3 小图所示,本研究测得的单位面积热导值在  $10^8\ \text{W}/(\text{m}^2 \cdot \text{K})^{-1}$  的数量级,与文献[1]中 1 nm 单壁碳纳米管接触节点热导值  $2.11 \times 10^8\ \text{W}/(\text{m}^2 \cdot \text{K})^{-1}$  以及文献[14]中 121 nm 和 74 nm 的多壁碳纳米管的接触热导在一个数量级,但比文献[1]中的分子动力学的模拟值  $3.5 \times 10^9\ \text{W}/(\text{m}^2 \cdot \text{K})^{-1}$  和文献[15]和[16]中的热导低一个数量级。值得注意的是,本研究 and 文献[1]的结果中:块状材料计算得到的热导值要比数值模拟及实验测得的单个碳纳米管接触节点热导明显小很多。本研究分析认为该现象可能与碳纳米管堆积床的特殊的三维网络拓扑结构有关。

图 6 为样品导热松弛时间的结果。 $\tau$  的值在测量范围内从 65 - 260 s,并且随着温度的升高而减少。关于非均匀的多孔介质具有较大的松弛时间的现象早已有报道。但此前文献报道最大的松弛时间也只有 10 s 的数量级,比本研究在碳管床中观测到的松弛时间要低一个数量级。该结果表明纳米颗粒堆积结构可能产生巨大的松弛时间。为进一步研究碳管接触节点上的瞬态热传导现象,采用 Cattnaeo-Nernotte 模型对碳纳米管床宏观导热进行分析。

$$q + \tau \frac{\partial q}{\partial t} = -k \frac{dT}{dx} \tag{7}$$

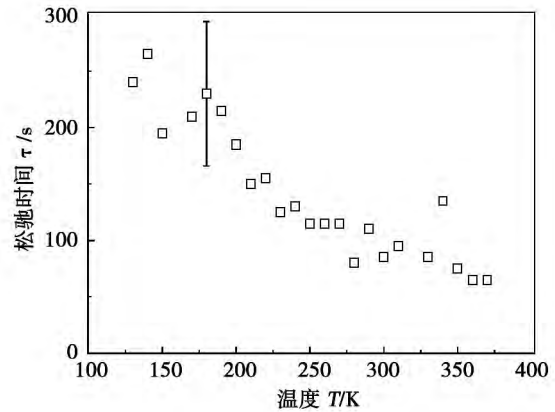


图 6 松弛时间随温度变化

Fig. 6 Changes of the relaxation time with temperature

将碳纳米管框架划分为多个基本单元,每一个基本单元内仅含有一个接触节点。根据之前的计算,碳管框架中空气的导热系数对碳管床有效导热系数影响可以忽略不计,则通过每个基本单元的热流等于通过碳纳米管接触点的热流。于是对于每个基本单元方程(7)可以改写为:

$$Q + \tau \frac{\partial Q}{\partial t} = G \Delta T \tag{8}$$

式中:  $Q = qA$ ,  $A$ —基本单元垂直于热流的面有效面积;  $\Delta T$ —两根碳纳米管接触点上温度差。式(8)给出了两根碳纳米管在接触节点上的瞬态热传导方程。由式(8)可以看出,单个碳纳米管接触节点间的传热松弛时间与块状试样中的松弛时间相等,碳管接触节点间具有同样巨大的松弛时间。因此,碳纳米管堆积床的松弛时间可能与碳纳米管之间纳米级接触节点的尺寸效应有关。假设相接触的两根碳纳米管的温度值分别恒定为  $T_1$  和  $T_2$ ,可得到通过接触节点的瞬态热流:

$$Q = G \Delta T (1 - e^{-t/\tau}) \tag{9}$$

式中:  $G$ —接触点处的热导,  $\Delta T = T_1 - T_2$ 。

图 7 为不同的松弛时间下接触点的热流随时间的变化,其中热流在瞬态热传导过程中显示出明显的延迟行为。由于松弛时间的存在,热流增加到稳态热流需要经过一段时间,并且松弛时间越大,时间越长。从这种延迟行为可以得到一个有趣的现象:两根碳管的温差一定,在一定时间范围内,存在较大松弛时间时瞬态导热热流要比稳态导热热流小很多。而热电势的大小只与温差有关,也即与稳态

的方法相比,使用上述的瞬态的方法可以消耗更少的热量来提供和维持相同的温差,从而获得同样的电能。这一现象的发现可能为热电的应用带来一种提高热电转换效率的新思路。

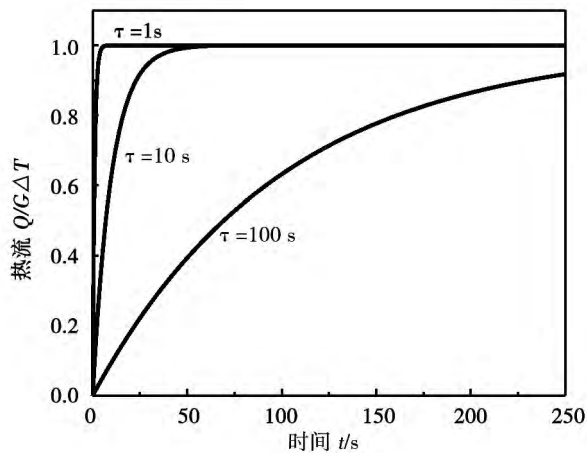


图7 不同松弛时间下纳米管接触节点之间的热流随时间的变化曲线。两根碳管温度恒定保持在  $T_1$  和  $T_2$

Fig. 7 Curves showing changes of the heat flux with time between the contact nodes of the nanometer tubes at various relaxation times. The temperatures of the two carbon tubes are constantly kept at  $T_1$  and  $T_2$  respectively.

### 3 结论

采用瞬态热线法测量碳纳米管堆积床从 120 – 370 K 温度范围内的导热系数和松弛时间,并结合 CV 模型分析了单个碳纳米管接触节点上的瞬态导热和热电特性,得出结论:

(1) 碳纳米管堆积床具有极低的导热系数,且导热系数在低于室温段随温度的升高线性增加,而在高于室温段趋于不变,该趋势与碳纳米管节点接触热导随温度的变化有关。

(2) 碳纳米管堆积床具有巨大的传热松弛时间,比此前文献报道的非均匀多孔材料的最大松弛时间还要高近一个数量级。

(3) 所观测到的松弛时间可能与碳纳米管之间接触节点上的尺寸效应有关。

(4) 这种多孔介质里的传热松弛时间带来的延迟效应可能提供一种新的利用纳米尺度材料提高热电效应的方法。

### 参考文献:

- [1] PRASHER R S, HU X J, CHALOPIN Y, et al. Turning Carbon Nanotubes from Exceptional Heat Conductors into Insulators [J]. *Physical Review Letters* 2009, 102(10): 105901 – 105904.
- [2] PRASHER R. Ultralow thermal conductivity of a packed bed of crystalline nanoparticles: A theoretical study [J]. *Physical Review B* 2006, 74(16): 165413.
- [3] HU X J. Ultralow thermal conductivity of nanoparticle packed bed [J]. *Appl Phys Lett* 2007, 91(20): 203113.
- [4] PADTURE N P, GELL M, JORDAN E H. Thermal Barrier Coatings for Gas-Turbine Engine Applications [J]. *science*, 2002, 296(5566): 280 – 284.
- [5] KELLY M J, WOLFE D E, SINGH J, et al. Thermal Barrier Coatings Design with Increased Reflectivity and Lower Thermal Conductivity for High-Temperature Turbine Applications [J]. *International journal of applied ceramic technology* 2006, 3(2): 81 – 93.
- [6] HOCHBAUM A I, CHEN R, DELGADO R D, et al. Enhanced thermoelectric performance of rough silicon nanowires [J]. *Nature*, 2008, 451(7175): 163 – 167.
- [7] VENKATASUBRAMANIAN R, SHIVOLA E, COLPITTS T, et al. Thin-film thermoelectric devices with high room-temperature figures of merit [J]. *Nature* 2001, 413(6856): 597 – 602.
- [8] HARMAN T C, TAYLOR P J, WALSH M P, et al. Quantum Dot Superlattice Thermoelectric Materials and Devices [J]. *science*, 2002, 297(5590): 2229 – 2232.
- [9] HSU K F. Cubic AgPbmSbTe<sub>2</sub> + m: Bulk Thermoelectric Materials with High Figure of Merit [J]. *science* 2004, 303: 818.
- [10] POUDEL B, HAO Q, MA Y, et al. High-Thermoelectric Performance of Nanostructured Bismuth Antimony Telluride Bulk Alloys [J]. *science* 2008, 320(5876): 634 – 638.
- [11] WANG X W, LEE H, LAN Y C, et al. Enhanced thermoelectric figure of merit in nanostructured n-type silicon germanium bulk alloy [J]. *Applied Physics Letters* 2008, 93(19): 193121 – 193123.
- [12] JOSHI G, LEE H, LAN Y C, et al. Enhanced Thermoelectric Figure-of-Merit in Nanostructured p-type Silicon Germanium Bulk Alloys [J]. *Nano Lett* 2008, 8(12): 4670 – 4674.
- [13] KO D-K, KANG Y, MURRAY C B. Enhanced Thermopower via Carrier Energy Filtering in Solution-Processable Pt – Sb<sub>2</sub>Te<sub>3</sub> Nanocomposites [J]. *Nano Lett* 2011, 11: 2841 – 2844.
- [14] YANG J, WALTERMIRE S, CHEN Y, et al. Contact thermal resistance between individual multiwall carbon nanotubes [J]. *Applied Physics Letters* 2010, 96(2): 023109 – 023113.
- [15] CHALOPIN Y, VOLZ S, MINGO N. Upper bound to the thermal conductivity of carbon nanotube pellets [J]. *Journal of Applied Physics* 2009, 105(8): 084301 – 084305.
- [16] ZHONG H, LUKES J R. Interfacial thermal resistance between carbon nanotubes: Molecular dynamics simulations and analytical thermal modeling [J]. *Physical Review B* 2006, 74(12): 125403.
- [17] VOLKOV A N, ZHIGILEI L V. Scaling laws and mesoscopic modeling of thermal conductivity in carbon nanotube materials [J]. *Physical Review Letters* 2010, 104(21): 215902.
- [18] NAN C W, SHI Z, LIN Y. A simple model for thermal conductivity of carbon nanotube-based composites [J]. *Chemical Physics Letters* 2003, 375(5–6): 666 – 669.
- [19] NAN C-W, LIU G, LIN Y, et al. Interface effect on thermal conductivity of carbon nanotube composites [J]. *Applied Physics Letters* 2004, 85(16): 3549 – 3551.
- [20] BARLETTA A. Hyperbolic propagation of an axisymmetric thermal signal in an infinite solid medium [J]. *International Journal of Heat and Mass Transfer*, 1996, 39(15): 3261 – 3671.

(陈滨 编辑)

factors being taken into account in a comprehensive way ,the lateral and longitudinal spacing of the spirally grooved tube bundles should be chosen as  $s_1 = 1.75$  to  $2 d$  and  $s_2 = 1.5$  to  $1.75 d$  respectively and the pitch should be chosen as  $P = 25$  to  $30$  mm while the groove depth should be chosen as  $e = 0.4$  to  $1$  mm. **Key Words:** spirally grooved tube , lateral/longitudinal spacing , pitch , groove depth , convection-based heat exchange outside tubes , heat transfer enhancement

**变密度多孔介质强化导热模型及实验研究 = Model for the Enhanced Heat Conduction of a Variable Density Porous Medium and Its Experimental Study** [刊 汉] YANG Li-hong , SUN Jin-xiang , SHEN Hang-ming ( College of Mechanical Engineering , Shanghai University of Science and Technology , Shanghai , China , Post Code: 200093) // Journal of Engineering for Thermal Energy & Power. - 2014 29( 5) . - 515 - 520

With the section of an isothermal vessel serving as the object of study ,based on the model for porous media ,the vessel was filled at a variable density to enhance the heat conduction from the center to the wall of the vessel. Firstly , based on a model for the minimized heat resistance of the heat conduction in the steady state ,the two-layer and three-layer copper wire filling scheme at a variable density were determined. Secondly , a test rig was set up according to the layered filling scheme and the effective heat conduction coefficient of the vessel was determined. Compared with the uniform filling scheme ,the heat conduction coefficient increased by 52.9% and 77.9% respectively. Finally , a numerical simulation study was performed of the transient heat conduction under the condition of the vessel being filled at a variable density. Under the condition of the central temperature being  $200$  °C and the central thermal power being constant ,through the heat conduction for a certain time period ,the filling at a variable density minimized the temperature difference between the center and wall of the vessel. The foregoing research results show that based on the minimized heat resistance ,layered filling with copper wires at a variable density can enhance the heat conduction from the center to its surroundings. **Key Words:** isothermal vessel , porous medium , variable density , enhanced heat conduction , effective heat conduction coefficient

**碳纳米管堆积床导热及热松弛 = Heat Conduction and Thermal Relaxation of a Carbon Nano-tube Pile-up Bed** [刊 汉] KAN Wei-min , XIAO Xiao-qing ( Guangdong Academy of Electric Power Sciences , Guangzhou , China , Post Code: 510600) , ZHANG Xian-tao , CHENG Ting ( College of Power and Mechanical Engineering , Wuhan University , Wuhan , China , Post Code: 430072) // Journal of Engineering for Thermal Energy & Power. - 2014 29( 5) . - 521 - 525

By employing the hot-wire method ,tested and measured were the heat conduction coefficient and heat transfer relax-

ation time of a carbon nano-tube pile-up bed within its temperature range ( 120K-370K) . The measurement data show that the heat conduction coefficient of the bed in question is extremely low. Its temperature rise in the low temperature section assumes a linear increase and that in the temperature range above the room temperature tends to be constant. During the measurement ,the carbon nano-tube bed indicated an evident heat transfer relaxation time , which was bigger than by a magnitude that of maximal carbon nano-tube bed reported by literatures currently available. On the basis of this datum and in combination with the classic Cattaneo-Vermotte ( CV) model ,the transient heat conduction and thermoelectric characteristics of a single carbon nano-tube in the contact node was analyzed. The research results show that by utilizing the heat conduction retarding characteristics of nano porous materials ,the transient thermoelectric conversion efficiency can be enhanced. **Key Words:** nano-composite material ,carbon nano-tube bed ,relaxation time ,heat conduction coefficient ,thermal power

300 MW 循环流化床锅炉动态特性的试验研究 = **Experimental Study of the Dynamic Characteristics of a 300 MW Circulating Fluidized Bed Boiler** [刊 ,汉] LI Peng-fei ,Ding Chang-fu ( College of Energy Source and Mechanical Engineering ,North China University of Electric Power ,Baoding ,China ,Post Code: 071003) ,ZHAO Ming ,SAI Jun-cong ( Yunnan Electric Power Experiment Research Institute ( Group) Co. Ltd. ,Electric Power Academy ,Kunming ,China ,Post Code: 650217) //Journal of Engineering for Thermal Energy & Power. - 2014 ,29 ( 5) . - 526 - 531

On the basis of the on-the-spot test of a 300 MW circulating fluidized bed boiler ,studied were the stepped response to the bed temperature and pressure of the circulating fluidized bed boiler with primary air quantity ,secondary air quantity ,coal feeding quantity and the opening degree of the material returning valve as well as the stepped response to the load of the boiler. By utilizing the particle swarm optimization algorithm-based intelligent identification ,a model for stepped response to the bed temperature ,bed pressure and boiler load under various operating conditions was established. The analytic results were kept in agreement with the theoretical simulation results studied previously by scholars ,thus offering reference and an underlying basis for optimization of the control tactics for the combustion systems of 300 MW circulating fluidized bed boilers and their operation at various loads. **Key Words:** circulating fluidized bed boiler ,bed temperature ,bed pressure ,dynamic characteristics

滚筒冷渣机中的颗粒径向扩散运动研究 = **Study of the Radial Diffusion Movement of Particles in a Roller Type Slag Cooler** [刊 ,汉] LU Chun-wang ,TAN Pei-lai ,LIU Bai-qian ,ZHU Xiao-long ( College of Mechanical Engineering ,Beijing University of Science and Technology ,Beijing ,China ,Post Code: 100083) //Journal of Engineering for Thermal Energy & Power. - 2014 ,29( 5) . - 532 - 538